



## MIDDLE EOCENE CLIMATIC OPTIMUM (MECO) IN THE MONTE CAGENERO SECTION, CENTRAL ITALY

Jairo F. Savian<sup>1,2\*</sup>, Luigi Jovane<sup>3</sup>, Ricardo I.F. Trindade<sup>1</sup>, Fabrizio Frontalini<sup>4</sup>, Rodolfo Coccioni<sup>4</sup>, Steven M. Bohaty<sup>5</sup>, Paul A. Wilson<sup>5</sup>, Fabio Florindo<sup>6</sup>, Andrew Roberts<sup>7</sup>

<sup>1</sup> Universidade de São Paulo, Instituto de Astronomia, Geofísica e Ciências Atmosféricas, São Paulo, Brazil

<sup>2</sup> Universidade Católica de Santos, Instituto de Pesquisas Científicas e Tecnológicas, Santos, Brazil

<sup>3</sup> Universidade de São Paulo, Instituto Oceanográfico, São Paulo, Brazil

<sup>4</sup> Università degli Studi di Urbino “Carlo Bo”, Urbino, Italy

<sup>5</sup> University of Southampton, National Oceanography Centre Southampton, Southampton, UK

<sup>6</sup> Istituto Nazionale di Geofisica e Vulcanologia, Rome, Italy

<sup>7</sup> The Australian National University, Canberra, Australia

### ABSTRACT

During the middle Eocene the Earth's climatic system experienced the MECO event (~ 40.0 Ma); it was a greenhouse warming event, which consisted in an abrupt reversal along with a long-term cooling through the middle Eocene. We report results of high-resolution environmental and rock magnetic investigations at Monte Cagnero (MCA) sedimentary section, in northeastern Apennines (Italy). A significant increase in fine magnetic materials during the middle Eocene warming event was observed. The environmental magnetic measurements along the section indicate a mixture of low and high coercivity minerals that includes magnetite (dominant) and hematite. Our results suggest that increase in magnetic parameters during the MECO peak depend on particulate iron and organ carbon delivery in the Neo-Tethys Ocean.

**Keywords:** Eocene climate, MECO, Monte Cagnero, Stable Isotopes, Environmental Magnetism.

### RESUMEN

Durante el Eoceno medio el sistema climático de la Tierra experimentó el evento MECO (~ 40.0 Ma), un calentamiento por efecto invernadero que consistió en una abrupta reversión durante un extenso período de enfriamiento a través del Eoceno medio. En este trabajo se presentan los resultados de las investigaciones magnéticas ambientales de alta resolución y de magnetismo de roca en la sección sedimentaria de Monte Cagnero (MCA), en los Apeninos del Noreste (Italia). Se observa un aumento significativo de los materiales magnéticos finos durante el evento de calentamiento del Eoceno medio. Las mediciones magnéticas ambientales a lo largo de la sección indican una mezcla de minerales de alta y baja coercitividad, que incluyen fundamentalmente magnetita y hematita, en menor proporción. Los resultados sugieren que el aumento en los parámetros magnéticos durante el pico del MECO dependen de la presencia de hierro particulado y la entrada de carbono orgánico en el océano Neo-Tethys.

**Palabras clave:** Clima del Mioceno, MECO, Monte Cagnero, Isótopos Estables, Magnetismo Ambiental.

### Introduction

The long-term global cooling trend of the Eocene was interrupted by the Middle Eocene Climatic Optimum (MECO) (e.g. Zachos *et al.*, 2008). The MECO is a 500-ka warming event centered at ~40.0 Ma (base of Chron C18n.2n) well characterized by a distinct negative ~1.0-1.5‰ in  $\delta^{18}\text{O}$  recognized in the Atlantic, Pacific and Southern Ocean (fig. 1). Beginning with a steady decrease in  $\delta^{18}\text{O}$  of ~0.5‰ at ~40.6-40.5 Ma, the MECO shows a climax at ~40.0 Ma and returns to pre-event values within less than 100 kyrs (Bohaty



*et al.*, 2009; Edgar *et al.*, 2010). The whole negative  $\delta^{18}\text{O}$  excursion spanning the onset of the MECO and its peak was interpreted as an increase of  $\sim 4\text{--}6^\circ\text{C}$  both at the surface and intermediate oceanic deep waters (Bohaty *et al.*, 2009).

Carbon isotopic records also show a distinct behavior along the MECO. Differently from the prominent negative carbon isotopes excursions (CIEs) characterizing the Paleocene-Early Eocene hyperthermal events,  $\delta^{13}\text{C}$  shifts are subtle during the MECO (Bohaty *et al.*, 2009). The steady decrease in  $\delta^{18}\text{O}$  that characterizes the first phase of the event is accompanied by a small positive shift in  $\delta^{13}\text{C}$ . The positive shift in  $\delta^{13}\text{C}$  values ends simultaneously with the brief prominent negative  $\delta^{18}\text{O}$  excursion around the MECO climax peaking at  $\sim 40.0$  Ma. At this point almost all sites show a 0.5-1.0‰ short-lived negative CIE within  $\sim 50$  kyr (Bohaty *et al.*, 2009). CIEs of the same magnitude before the MECO climax have also been reported from high-resolution benthic foraminiferal record at equatorial latitudes and may be related to the shoaling of lysocline and of the carbonate compensation depth (CCD), similar to the hyperthermal events observed through the Early Eocene (Edgar *et al.*, 2010).

In order to investigate the MECO event within the Tethyan realm, here we present a complete high-resolution isotopic and magnetic record for Monte Cagnero (MCA) section from central Italy. The age model for MCA section is well constrained through high-resolution magnetostratigraphy and biostratigraphy (Jovane *et al.*, 2013), thus enabling the comparison of our results with the worldwide record of MECO from the Atlantic, Pacific and Southern Oceans (Bohaty *et al.*, 2009).

### Geological setting, materials and methods

The MCA section is exposed on the southeastern slope of Monte Cagnero (Lat.  $43^\circ 38' 50''$  N, Long.  $12^\circ 28' 05''$  E, 727 m above sea level) near the town of Urbania, northeastern Apennines (Italy) (fig. 1). Because of its completeness and continuity, the MCA represents an important sedimentary pelagic sequence to study the climatic events during Eocene and Oligocene Epochs (Coccioni *et al.*, 2008; Jovane *et al.*, 2013). In the present study, we will focus on the lower part of the section from 58 to 72 msl. This 14-m thick interval belongs to the Scaglia Variegata Formation that consists of bundles of limestone-marl couplets.

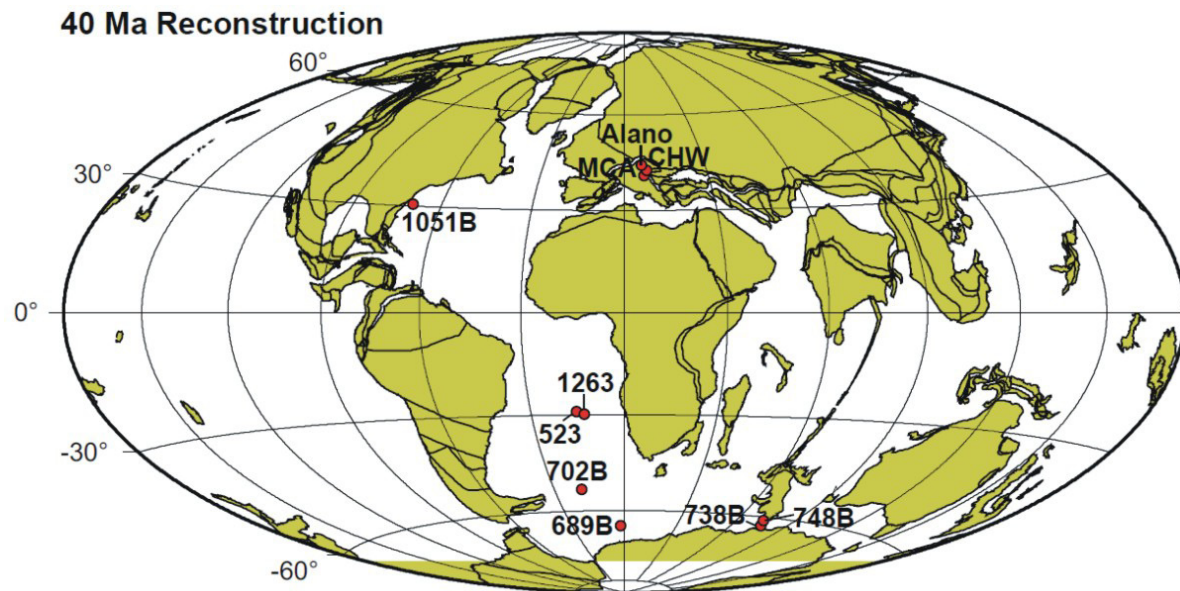


**Figure 1.** Site locations of middle Eocene IODP-ODP and land sections included the new MCA section. Palaeogeographic positions at 40 Ma are plotted on paleogeographic reconstruction generated from the Ocean Drilling Stratigraphic Network (GEOMAR, Kiel, Germany). Data are compiled from Jovane *et al.* (2007), Bohaty *et al.* (2009), Luciani *et al.* (2010), and Spofforth *et al.* (2010).

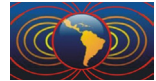


It was deposited at the same paleolatitude as CHW but at deeper depths (~1000-1500 m) (Guerrera *et al.*, 1988; Parisi *et al.*, 1988). The studied interval comprises the top of Chron C18r (40.79 Ma, 58.00 msl) until the base of Chron C18n (39.13 Ma, 72.00 msl) (Jovane *et al.*, 2013).

High-resolution calcium carbonate, carbon and oxygen isotopes and rock magnetic analyses were performed. Paleomagnetic measurements and environmental magnetism analyses were carried out at the National Oceanography Centre Southampton (NOCS), UK. Measurements were performed using a three-axis 2-G Enterprises cryogenic magnetometer (model 755R), housed in a magnetically shielded room. In order to obtain a quantitative inference of variation of the composition, concentration and grain-size of the magnetic minerals (*e.g.* Evans and Heller, 2003), we analysed the rock magnetic properties of 253 unoriented block samples (5-cm resolution).

The low field mass-specific magnetic susceptibility ( $\chi$ ) was measured with a Kappabridge KLY-4, AGICO magnetic susceptibility meter. An anhysteretic remanent magnetization (ARM) was imparted in a 100 mT AF with a superimposed 0.05 mT direct current (DC) bias field. An isothermal remanent magnetization (IRM) was imparted to the samples by applying a 900 mT direct field ( $IRM_{900\text{mT}}$ ). Then, it was imparted a backfield isothermal remanent magnetization (BIRM) at 100 mT ( $BIRM_{-100\text{mT}}$ ) and 300 mT ( $BIRM_{-300\text{mT}}$ ). From these measurements, we calculated S-ratios ( $S_{300\text{mT}} = [BIRM_{300\text{mT}}/IRM_{900\text{T}}]$ ) and hard isothermal remanent magnetization ( $HIRM_{300\text{mT}} = [IRM_{900\text{mT}} + BIRM_{300\text{mT}}]/2$ ), in order to investigate the coercivity of the magnetic minerals. The ARM activates the finer magnetic grains, whereas IRM activates the entire magnetic component. The HIRM provides information about the magnetic coercivity of the magnetic carriers. The presence of low coercivity magnetic mineral (*e.g.*, magnetite) is indicated by the value of S-ratio<sub>300mT</sub> close to unity. In contrast, low S-ratio<sub>300mT</sub> values and high values of HIRM<sub>300mT</sub> indicate the presence of high-coercivity magnetic minerals (*e.g.*, hematite). The two latter parameters indicate both a subtle variation in the composition of magnetic minerals as well as a non-significant variation in grain size and concentration. Magnetic mineralogy also was investigated through acquisition of isothermal remanent magnetization (IRM) in a 2G pulse magnetizer, while remanence measurements were performed with the 2G-cryogenic magnetometer from the University of São Paulo (USP), Brazil. IRM acquisition curves were separated into different coercivity components (Robertson and France, 1994) and were obtained at fields up to 1 T for six representative samples and analyzed by cumulative log-Gauss function (CLG) using the software developed by Kruiver *et al.* (2001). The CLG function is described by three optimal parameters (M<sub>ri</sub>, B<sub>1/2</sub> and dispersion parameter, DP) that characterize each magnetic carrier of the sample (Robertson and France, 1994; Kruiver *et al.*, 2001). In order to determine the Curie or Néel (temperature above which collective magnetic ordering is overcome by thermal energy and the mineral becomes paramagnetic) temperature of the magnetic minerals were used high-thermomagnetic curves (susceptibility vs. temperature). For selected samples, thermomagnetic curves during heating to 700 °C were obtained using a KLY-3 magnetic susceptibility meter (AGICO) at the Paleomagnetic Laboratory, USP.

For selected samples at MCA section,  $\delta^{18}\text{O}$  and  $\delta^{13}\text{C}$  analyses were conducted using VG Optima and VG Prism dual-inlet isotope ratio mass spectrometers at the NOCS. The samples were reacted in a common acid bath maintained at 90 °C using an automated carbonate preparation system with a carousel device. NBS-19, Atlantis II, and an in-house Carrara marble standard were included in all sample runs. All values are reported in standard delta notation ( $\delta$ ) in parts per mil (‰) relative to VPDB (Vienna Pee Dee Belemnite), and analytical precision is estimated at 0.06‰( $1\sigma$ ) for  $\delta^{13}\text{C}$  and 0.08‰( $1\sigma$ ) for  $\delta^{18}\text{O}$ . Analyses of carbonate content were performed at the geochemistry laboratory of NOCS. The bulk rock samples were reduced to fine powder in an agate mortar. Calcium carbonate content measurements were obtained using a Dietrich-Fruhling calcimeter. The method is based on the measurement of CO<sub>2</sub> volume produced by the complete dissolution of pre-weighted samples (300±1 mg each) in 10% vol. HCl. Total carbonate contents (wt.% CaCO<sub>3</sub>) were computed with a precision of 1% using formulae that take into account pressure and temperature of the lab environment, amount of bulk sample used, and the volume of CO<sub>2</sub> developed in the calcimeter. Standards of pure calcium carbonate (*e.g.*, Carrara Marble) were measured every ten samples to ensure proper calibration.



## Results and Analysis

The MECO event is recognized by its distinct oxygen isotopic excursion of 1.0-1.5‰ for bulk and fine carbonate fractions (figs. 2D-J). MCA section show very noisy oxygen isotope data that significantly differ

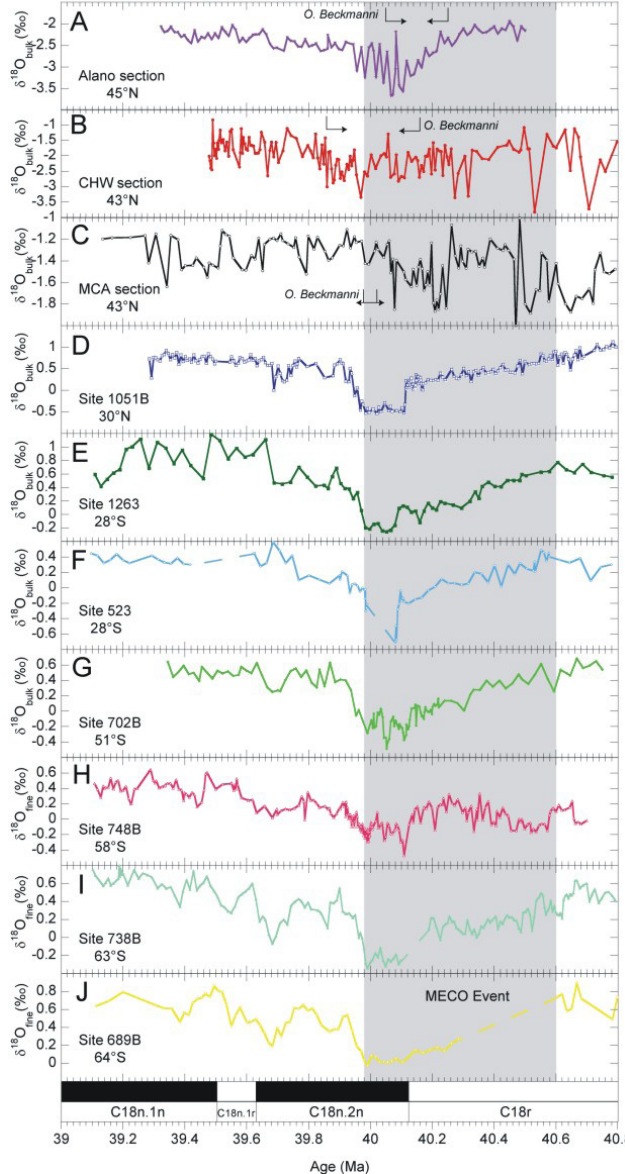


**Figure 2.** Compilation of Neo-Tethys Ocean bulk-sediment oxygen isotope ( $\delta^{18}\text{O}$ ) records between 40.8 and 39.0 Ma from Alano, CHW and MCA sections and stable oxygen isotope data compiled for Sites 1051B, 1263, 523, 702B, 748B, 738B, and 689B, which range geographically from the midlatitude North Atlantic to high latitudes of the Atlantic Ocean and Indian Ocean sectors of the Southern Ocean. The age model for the sections is based on magnetostratigraphy. A prominent decrease in  $\delta^{18}\text{O}$  values at 40.0 Ma is observed at all ODP Sites, but not observed in Tethyan section. The area shaded in light grey denotes the MECO event previously defined by Bohaty *et al.* (2009).

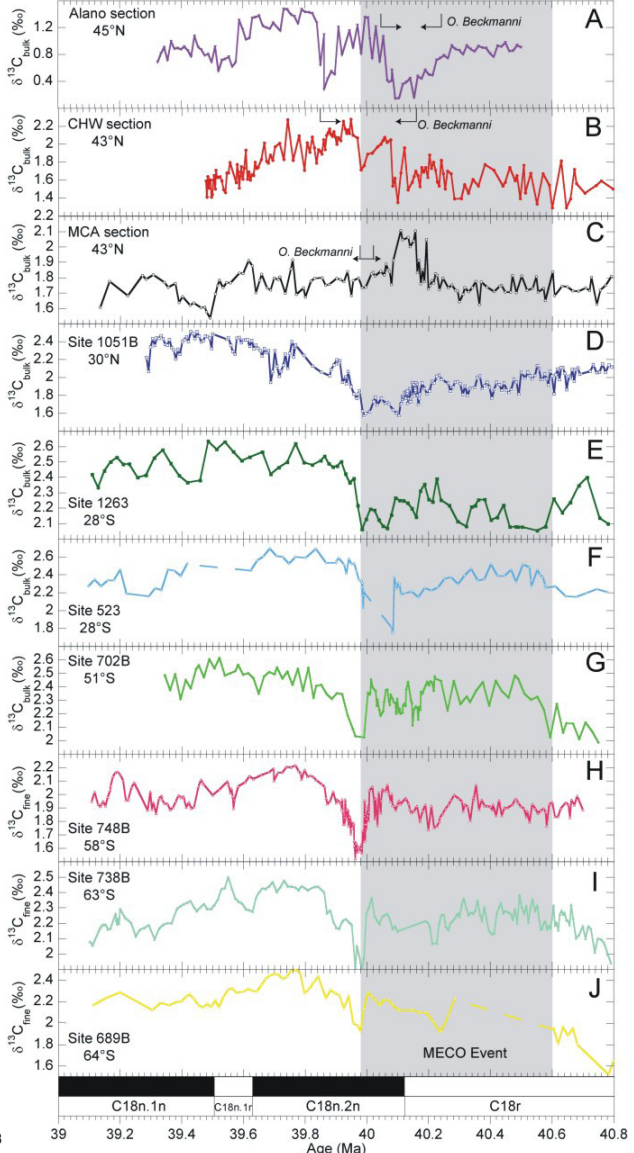


**Figure 3.** Bulk-sediment carbon isotope ( $\delta^{13}\text{C}$ ) records for the middle Eocene interval between 40.8 and 39.0 Ma from Alano, CHW and MCA sections. Bulk-sediment and fine-fraction carbon isotope ( $\delta^{13}\text{C}$ ) records for the middle Eocene interval, between 40.8 and 39.0 Ma; previously published by Bohaty *et al.* (2009). The area shaded in light grey denotes the MECO event previously defined by Bohaty *et al.* (2009).



from the record of sections outside the Tethys (figs. 2A-C). Bulk  $\delta^{18}\text{O}$  MCA section (fig. 2C) varying from -2.0‰ to -1.0‰, with no clear correlation between sections. The bulk  $\delta^{13}\text{C}$  data from MCA section (fig. 3C) show a prominent peak between 40.29 Ma and 40.15 Ma from background values of ~1.8‰ to maximum values of ~2.1‰. The peak value is followed by a smooth decrease trend up to ~39.8 Ma. This excursion is associated to an increase in organic matter content in the section and a decrease in  $\text{CaCO}_3$  (from ~80-90% to ~47-60% during the isotopic excursion), as well as an increase in magnetic parameters, suggesting it is a local effect associated to higher productivity.

The calcium carbonate content record has an average value of ~80% (minimum ~46.7% and maximum ~92.96% at 63.25 msl and 61.80 m, respectively) (fig. 4a). Two discrete intervals (63-63.55 msl and 64.15-65.30 msl) containing lower carbonate contents and higher values of low-field magnetic susceptibility ( $\chi$ ) are recognized (fig. 5a). The  $\chi$  profile displays values between  $0.57 \times 10^{-6}$  to  $6.42 \times 10^{-6}$  SI/g (fig. 5a). Calcium

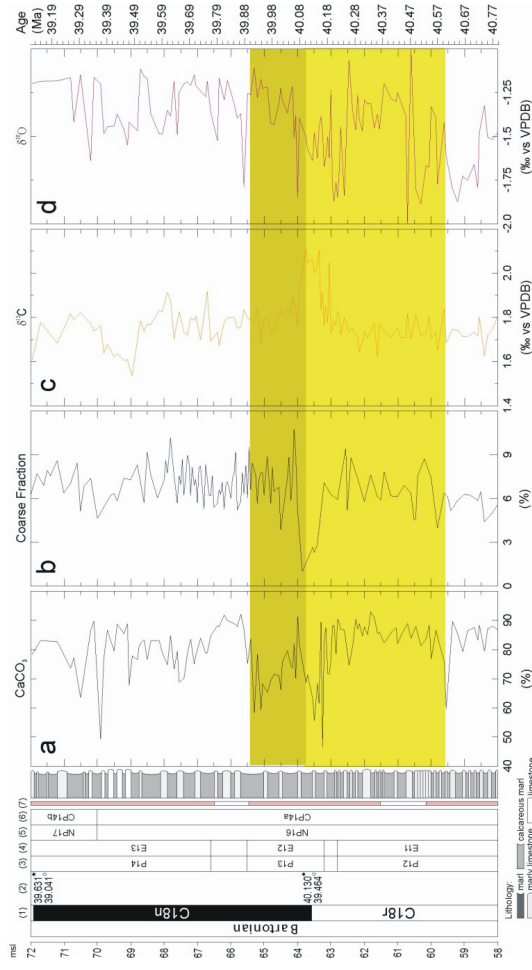


**Figure 4.** Changes in  $\text{CaCO}_3$  content, coarse fraction,  $\delta^{18}\text{O}$  and  $\delta^{13}\text{C}$  in bulk sediments across the 14 m-thick studied segment at MCA section. The area shaded in yellow highlights and dark yellow represents the interval of warming during the MECO and peak of the event based on Bohaty *et al.* (2009).

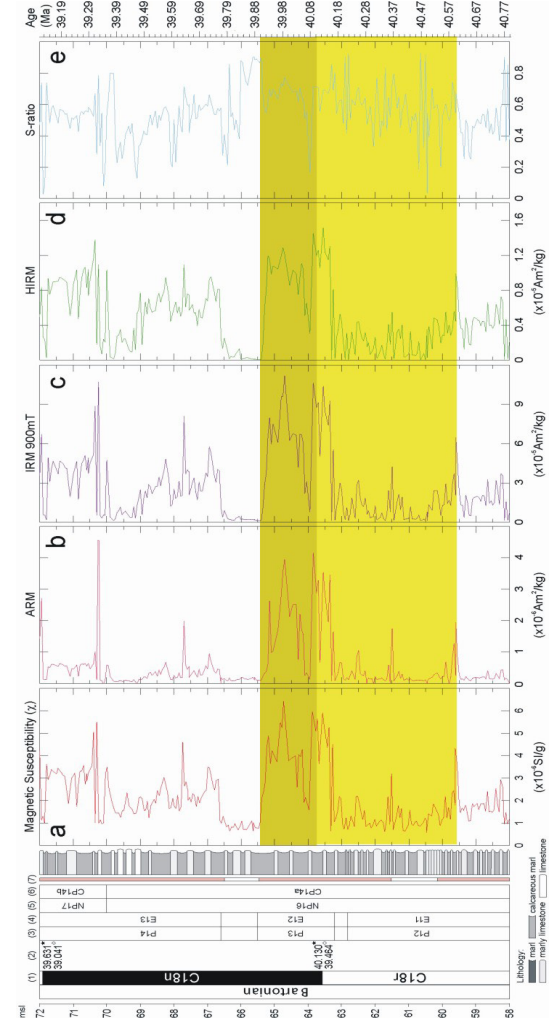
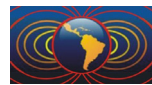


**Figure 5.** Low-field magnetic susceptibility ( $\chi$ ), and rock magnetic properties across the 14 m-thick studied segment at MCA section. Magnetic properties: anhysteretic remanent magnetization, ARM; isothermal remanent magnetization, IRM at 900mT; hard isothermal remanent magnetization, HIRM; S-ratio300mT. The area shaded in yellow highlights and dark yellow represents the interval of warming during the MECO and peak of the event based on Bohaty *et al.* (2009).



carbonate and  $\chi$  records show a significant negative correlation ( $r = -0.72$ ). Relatively high values of  $\chi$  are related to low values of  $\text{CaCO}_3$  and correspond to peaks in abundance of paramagnetic (e.g., increased amount of clay minerals) and ferromagnetic minerals in the sediments. The coarse fraction record shows a marked decrease from ~62.5 to 64.0 msl (fig. 4b).

The rock magnetic properties exhibit marked changes along the studied segment (fig. 5). The ARM shows an average value of  $5.70 \times 10^{-7} \text{ Am}^2/\text{kg}$ , minimum of  $1.14 \times 10^{-9}$  and maximum of  $6.66 \times 10^{-6} \text{ Am}^2/\text{kg}$  (fig. 5b). In the interval where were observed the peak in  $\chi$ , the ARM also increase. When the magnetic mineralogy changes, ARM increase reflects fine magnetic grain size (Thompson and Oldfield, 1986). The IRM ranges from  $1.11 \times 10^{-6}$  to  $1.12 \times 10^{-4} \text{ Am}^2/\text{kg}$  with an arithmetic mean of  $2.47 \times 10^{-5} \text{ Am}^2/\text{kg}$  (fig. 5c). The  $\text{HIRM}_{300T}$  ranges from  $4.19 \times 10^{-8}$  to  $7.51 \times 10^{-4} \text{ Am}^2/\text{kg}$  with an arithmetic mean of  $1.61 \times 10^{-5} \text{ Am}^2/\text{kg}$  (fig. 5d). The S-ratio varies from 0.03 to 0.93 m with an arithmetic mean of 0.54 (fig. 5e). S-ratio indicates that the magnetic mineral assemblage is dominated by a complex mixture of low and high-coercivity magnetic minerals, which includes magnetite and/or maghemite (predominant) and hematite.

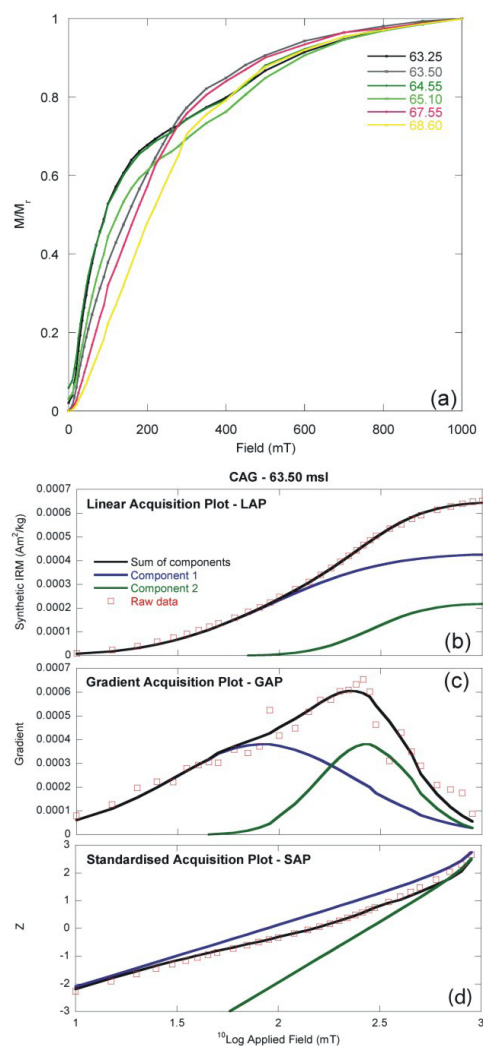
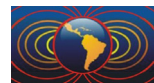


**Figure 6.** IRM acquisition curves for six representative samples from Monte Cagnero section, and example of LAP-GAP-SAP analysis of sample 63.50 msl obtained using the software developed by Kruiver *et al.* (2001).

Isothermal remanent magnetization acquisition curves were obtained at fields up to 1 T for 6 representative samples along the 14 m-thick of the MCA section (fig. 6a) and analyzed by cumulative log-Gauss functions (CLG) (fig. 6b-d). Three magnetic components are identified in only one studied sample (64.55 msl). For the other 5 representative samples, the CLG models were fitted with two components for each sample suggesting two magnetic carriers. SIRM,  $B_{1/2}$  and DP values indicate low- to medium-coercivity magnetic carriers for the component 1 (Robertson and France, 1994). The lowest coercivity component 1 is interpreted to fine-grained magnetite. The highest coercivity component (component 2) is dominated by a magnetic mineral with high coercivity (e.g. Hematite). The low-coercivity magnetic mineral is dominant (between 57.9% to 72.6%) in all studied samples along the interval.  $\chi$ -T curves indicate that magnetite is the dominant magnetic mineral (fig. 7).

## Conclusions

We performed multidisciplinary study on 14 m-thick section at Monte Cagnero (Umbria-Marche Basin) corresponding to a time interval between 40.79 and 39.12 Ma. Continue high-resolution stable isotopes and environmental magnetism parameters have been produced in conjunction with selected rock magnetic measurements. On the bases of IRMs acquisition curves, it was possible to recognize the presence of SD non-interactive magnetite, which provides further evidence of magnetofossils presence in the sediments (e.g., Roberts *et al.*, 2011; Larrasoña *et al.*, 2012). This finding allows us to infer that the MECO climax and the aftermath of MECO are high productivity phases when Tethyan deep waters and sediments



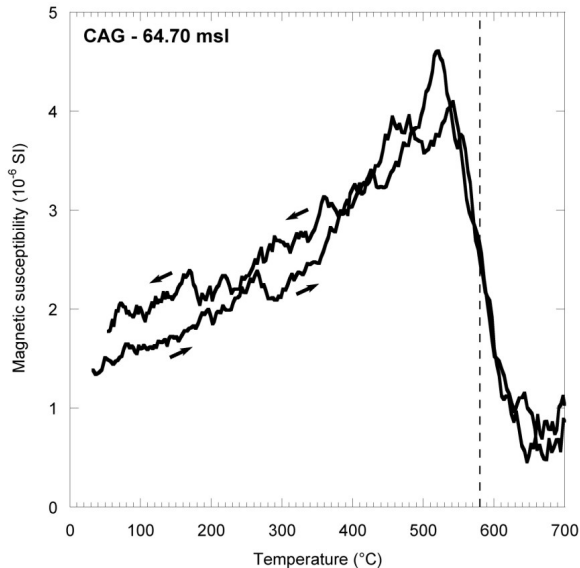
where under suboxic conditions. We are the first to testify that the MECO event is associated to a phase of high-productivity and an increase of suboxic conditions in deep-sea environments. Moreover, we also obtain the first proof that magnetization in deep sediments when kept by magnetofossils could represent an important climatic and environmental proxy.

### Acknowledgements

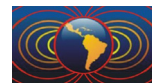
We would like to thank the financial support provided by Marie Curie Actions (FP7-PEOPLE-IEF-2008, proposal n. 236311). Jairo F. Savian acknowledges the Brazilian CNPq (Process 201508/2009 5) for funding a Visiting Fellowship at the National Oceanography Centre Southampton (NOCS), where the magnetic and isotopic studies were completed.

### References

- Bohaty, S. M., Zachos, J. C., Florindo, F. and Delaney, M. L., 2009. Coupled greenhouse warming and deep-sea acidification in the middle Eocene. *Paleoceanography*, 24, PA2207, doi:10.1029/2008PA001676.
- Coccioni, R., Marsili, A., Montanari, A., Bellanca, A., Neri, R., Bice, D. M., Brinkhuis, H., Church, N., Macalady, A., McDaniel, A., Deino, A., Lirer, F., Sprovieri, M., Maiorano, P., Monechi, P., Nini, C., Nocchi, M., Pross, J., Rochette, P., Sagnotti, L., Tateo, F., Touchard, Y., Van Simaeys, S., Williams, G. L., 2008. Integrated stratigraphy of the Oligocene pelagic sequence in the Umbria-Marche basin (northeastern Apennines, Italy): a potential Global Stratotype Section and Point (GSSP) for the Rupelian/Chattian boundary. *Geol. Soc. Am. Bull.* 120, 487–511.
- Edgar, K. M., Wilson, P. A., Sexton, P. F., Gibbs, S. J., Roberts, A. P. and Norris, R. D., 2010. New biostratigraphy, magnetostratigraphy and isotopic insights into the Middle Eocene Climatic Optimum in low latitudes. *Palaeogeogr. Palaeoclimatol. Palaeoecol.*, 297, 670-682.
- Evans, M. E., Heller, F., 2003. Environmental magnetism: Principles and applications and enviromagnetics. *International Geophysics Series*, v. 86, edited by R. Dmowska, J.R. Holton, and H.T. Hossby. Academic Press, Elsevier.
- Guerrera, F., Monaco, P., Nocchi, M., Parisi, G., Franchi, R., Vannucci, S., Giovannini, G., 1988. La Scaglia Variegata Eocenica nella sezione di Monte Cagnero (bacino marchigiano interno): studio litostratigrafico, petrografico e biostratigrafico. *Bull. Soc. Geol. Ital.* 107, 81–99.
- Jovane, L., Florindo, F., Coccioni, R., Dinarès-Turell, J., Marsili, A., Monechi, S., Roberts, A.P., Sprovieri, M., 2007. The middle Eocene climatic optimum (MECO) event in the Contessa Highway section, Umbrian Apennines, Italy. *Geol. Soc. Am. Bull.* 119, 413–427, doi: 10.1130/B25917.1.
- Jovane, L., Savian, J. F., Coccioni, R., Frontalini, F., Bancalà, G., Catanzariti, R., Luciani, V., Bohaty, S. M., Wilson, P. A., Florindo, F., 2013. Integrated magnetobiostratigraphy of the middle Eocene-Oligocene interval from the Monte Cagnero section, central Italy. In: Jovane, L., Herrero-Bervera, E., Hinnov, L.A., Housen, B.A. (Eds.), Magnetic Methods and the Timing of Geological Processes. *Geol. Soc. Lond. Spec. Publ.* 373, doi:10.1144/SP373.13.



**Figure 7.** Thermomagnetic curve for a representative sample from 64.70 msl. This sample contains magnetite as dominant magnetic carrier (sharp decline in susceptibility to approximately 580° C). The susceptibility during the cooling cycle was not thermal altered during heating.



- Kruiver, P. P., Dekkers, M. J., Heslop, D., 2001. Quantification of magnetic coercivity components by the analysis of acquisition curves of isothermal remanent magnetization. *Earth Planet. Sci. Lett.*, 189, 269-276.
- Larrasoña, J. C., Roberts, A. P., Chang, L., Schellenberg, S. A., Fitz Gerald, J.D., Norris, R. D., Zachos, J. C., 2012. Magnetotactic bacterial response to Antarctic dust supply during the Paleocene-Eocene thermal maximum. *Earth Planet. Sci. Lett.* 333–334, 122–133.
- Luciani, V., Giusbert, L., Agnini, C., Fornaciari, E., Rio, D., Spofforth, D.J.A., Pälike, H., 2010. Ecological and evolutionary response of Tethyan planktonic foraminifera to the middle Eocene climatic optimum (MECO) from the Alano section (NE Italy). *Palaeogeogr. Palaeoclimatol. Palaeoecol.*, 292, 82–95.
- Parisi, G., Guerrera, F., Madile, M., Magnoni, G., Monaco, P., Monechi, S., Nocchi, M., 1988. Middle Eocene to early Oligocene calcareous nannofossil and foraminiferal biostratigraphy in the Monte Cagnero section, Piobbico (Italy). In: Premoli Silva, I., Coccioni, R., Montanari, A. (Eds). The Eocene/Oligocene boundary in the Marche-Umbria basin (Italy), International Subcommission on Paleogene Stratigraphy, Ancona.
- Roberts, A. P., Florindo, F., Villa, G., Chang, L., Jovane, L., Bohaty, S. M., Larrasoña, J.C., Heslop, D., Gerald., J. D. F., 2011. Magnetotactic bacterial abundance in pelagic marine environments is limited by organic carbon flux and availability of dissolved iron. *Earth Planet. Sci. Lett.* 310, 441-452.
- Robertson, D. J., France, D. E., 1994. Discrimination of remanence-carrying minerals in mixtures, using isothermal remanent magnetisation acquisition curves. *Phys. Earth Planet. Inter.* 84, 223-234.
- Spofforth, D. J. A., Agnini, C., Pälike, H., Rio, D., Fornaciari, E., Giusbert, L., Luciani, V., Lanci, L., Muttoni, G., 2010, Organic carbon burial following the middle Eocene climatic optimum in the central western Tethys. *Paleoceanography* 25, PA3210, doi:10.1029/2009PA001738.
- Thompson, R., Oldfield, F., 1986. Environmental Magnetism. Allen and Unwin, Winchester, Mass.
- Zachos, J. C., Dickens, G. R., Zeebe, R. E., 2008. An early Cenozoic perspective on greenhouse warming and carbon-cycle dynamics. *Nature* 451, 279–283.